Friction **12**(4): 683–697 (2024)
https://doi.org/10.1007/s40544-023-0784-0
ISSN 2223-7690
CN 10-1237/TH
RESEARCH ARTICLE

On the electric behaviour of conductive grease inside the contact zone

Yuxin ZHOU[1,*], Jinjie LIU[2], Xinming LI[2], He CHONG[1], Bo HAN[1], Qinghua BAI[2]

[1] *SKF (Shanghai) Automotive Technologies Co., Ltd., Shanghai 201814, China*

[2] *School of Mechanical and Automotive Engineering, Qingdao University of Technology, Qingdao 266250, China*

Received: 14 February 2023 / Revised: 04 May 2023 / Accepted: 22 May 2023

Abstract: Conductive grease has been considered as a potential solution in addressing electric erosion issue inside motor bearings. Understanding the conductive grease performance, especially the electric and tribological behaviour is crucial for its application. This paper combines bulk grease characterization and contact film study considering both electrical and tribological loading conditions. The results show that the electric performance for the selected conductive grease sample is electric field dependent, including both frequency and voltage amplitude. Its film impedance inside the contact area is closely related to the external electric field, running condition, and lubrication regime. The following film impedance calculation tells that not only bulk grease electric parameters, but the contact parameter, lubricant film contour and lubrication condition should be considered when performing the overall bearing electrical modelling.

Keywords: Electric erosion; lubricant conductivity; grease; film impedance

1 Introduction

Electric erosion is commonly observed inside the bearings due to the circumferential current and common mode voltage induced bearing current for a pulse width-modulation (PWM) inverter driving motor [1, 2]. Such discharge arcing will result in the local melting of raceway and rolling element (frosting and fluting), deterioration of the NVH performance, degradation of lubricant and the premature failure of bearing [3, 4]. To control the electric current damage in rolling bearings, different remediating methods have been tried, one is the insulating approach, e.g., hybrid bearings or insulating coating to cut the electric circuit [5]; the other is the conducting approach, where grounding ring [6], conductive seal [7] or bearing are applied to transfer the aggressive current. Among them, electric conductive grease has been a continuous interest to address the electric current damage as the accumulated voltage or bearing current is expected to be guided away from the shaft to the motor housing through the low electric resistant (conductive) lubricating film [8].

Conductive grease was initially developed for conductive parts of electrical machinery such as switches, integrated circuits [9], contact stripes of electrical locomotives [10], etc. Its electric conductivity originates from the conductive agents, e.g., metal powders [11], carbon nanotubes [12], graphene [13], ionic liquid [14], conductive polymer [15], etc. and there is a wealth of information on their chemical composition and tribological performance [16–18]. In some concepts, motor bearing was filled with conductive grease so as to transfer the electric current from the rotor to the grounding frame directly [15]. In another approach, a "rotor discharge bearing" packed with conductive grease was designed in the motor system to protect the main rotor bearing [19].

The electric field inside a PWM inverter driven motor shows a character of Alternating current (AC)

* Corresponding author: Yuxin ZHOU, E-mail: yuxin.zhou@skf.com.

voltage or current with high frequency [20] and variable amplitude generated from the parasitic capacitors inside the motor [3]. In addition, the expected electric channel for conductive grease is on the base of the lubricating film layer inside the contact zone. This film layer is always in a dynamic rather than steady state, which is highly related to load, speed, temperature, grease lubricity, lubricant replenishment, etc., causing a film evolution and complicated film constitution [21]. Such combined electrical and tribological environments complicates the evaluation of conductive grease performance in the bearing. Luo and Xie [22, 23] performed comprehensive tribological studies in thin film lubrication regime under external electrical load. According to their results, external electric field may result in film instability such as local discharge, electro-viscosity rising [24], microbubble [25], unstable lubricant flow, etc., but their study also confirmed these behaviours would differ for grease lubrication [26]. Other Direct current (DC) or AC electric powered fundamental tests can be found in the literature [27–32] as well, whilst the electric performance for conductive grease in a dynamic contact zone under high frequency AC electric environment still remains ambiguous.

This paper focuses on bridging the conductive grease electric behaviour to its tribological performance which may contribute to the development and application of conductive greases in addressing the electric erosion issues. In order to achieve this, not only the bulk grease analysis is in need, it is equally important to know its microscopic electric response inside the contact zone considering both mechanical and electrical loading parameters. The bulk grease electric behaviour is performed using an LCR metre and the film impedance is carried out using a ball-on-disc contact geometry with an LCR metre as the electric loading source. Finally, numerical film impedance is calculated using the electric volume impedance from the bulk analysis and the film thickness profile from the ball-on-disc test. The calculated film impedance is compared to the measured results to study the connection between the steady bulk grease analysis and the dynamic film layer behaviour in the contact zone.

2 Sample and Methodology

2.1 Tested sample

Two lubricating greases were selected as tested sample, labelled as CG (conductive grease) and NCG (non-conductive grease). To the authors' knowledge, CG and NCG share similar base oil and thickener, except that the ionic liquid was added to CG as the conductive agent. In addition to fresh sample, pre-treatment was carried out to reflect the degradation of grease inside a bearing: fresh CG and NCG were baked in a thermal chambre at 120 °C and 150 °C for 240 hours; also, fresh CG and NCG were mechanically aged inside a grease worker for 100,000 strokes. According to the grease lubricating mechanism, bled oil plays an important role in bearing lubrication and contact film construction [21]. To study the interaction between conductive agent and grease bled oil, and their contribution to grease electric performance in the contact zone, bled oil for CG and NCG were collected using the DIN51817-14 oil separation apparatus, but at 100 °C to accelerate the oil separation. The bled oils are termed as CGBO (conductive grease bled oil) and NCGBO (non-conductive grease bled oil), respectively. The tested sample properties and pre-treatment conditions are provided in Table 1.

2.2 Bulk grease analysis

Bulk grease electric analysis was carried out by measuring the grease impedance at ambient condition. Different from the electric conductivity evaluation using fixed voltage or current [33, 34], a Victor 4092E

Table 1 Tested sample information.

Fresh sample	CG	NCG
Base oil viscosity KV40 (cSt)	72	80
Base oil viscosity KV100 (cSt)	9.5	9.5
Thickener	Polyurea	Polyurea
Base oil	Ester	Ester
Conductive agent	Ionic liquid	No
Thermal baking at 120 °C (h)	240	240
Thermal baking at 150 (h)	240	240
Mechanical shear in grease worker	100,000 strokes	100,000 strokes
Bled oil collected from 100 °C test	CGBO	NCGBO

LCR metre was used to apply variable electrical parameters on the measuring subject. As the motor shaft voltage may fall in different frequency and amplitude ranges because of the various inverter switching frequency and parasitic capacitors [3], for each sample, frequency sweep was applied from 10 Hz up to 1 MHz (top limit of the current apparatus) with a default AC voltage amplitude at ±1 V. This frequency sweep test was performed using an Anton Paar 302e rheometer dielectric module, shown in Fig. 1, where the target samples (grease or oil) are packed between a pair of plate-plate geometry with 12.5 mm as radius, yielding a measuring area as $A_p = 4.91\times10^{-4}\,\mathrm{m}^2$, and at an accurately controlled measuring gap. The plate–plate geometry was subsequently connected to the LCR metre by a specific electric circuit and was isolated from the rest of the rheometer. The sample electric impedance was measured at steady state with a fixed measuring gap h_p = 0.5 mm. Different measuring gaps was also tried at 0.9 mm and 1.5 mm, giving different absolute impedance value but does not change the overall trend, and in the following test, 0.5 mm was selected for the sake of sample saving, especially the bled oil. The impedance parameters from the rheometer will be used in the following film impedance calculation.

In addition, a DC bias sweep was applied using an external DC power source. A DC amplitude sweep was set up to 50 V to study the grease behaviour at elevated voltage conditions. Unfortunately, the rheometer system cannot suffer such high amplitude, and thus a simplified measuring apparatus was used. As is schematically shown in Fig. 1, the sample was packed between two copper plates which were connected to the LCR metre, with a measuring gap at 0.5 mm as well fixed by a three-dimensional (3D) printed framework. The parallel frequency sweep tests between rheometer and this simplified measuring apparatus tell that, although the absolute values are different, the overall behaviour remains the same. Therefore, for the DC bias sweep test and the test for aged grease samples, the simplified test apparatus was used for the trend analysis. Each frequency or DC bias test was repeated twice. Also, to check the potential chemical reaction during the thermal baking and the electrical tests, Fourier Transform Infrared (FTIR) spectroscopy analysis was performed using a BRUKER Tensor 27 FTIR metre.

2.3 Grease tribological study

The grease film thickness was measured by optical interferometry method using an in-house made ball on disc test rig in the open air and its schematic drawing is shown in Fig. 2. The load of 30 N (equalling a maximum Hertz contact pressure of 0.5 GPa) was added by a pre-defined weight and a lever geometry; the ball and disc were driven by a motor and a spindle separately, and pure rolling condition was applied. In the current study, fully flooded condition was applied where the grease adjacent to the contact zone was collected and pushed back to the inlet area through a 3D printed "grease collector", giving a continuous inlet track width w_{in} = 2 mm and an inlet track height h_{in} = 0.5 mm. To cover a full range of lubrication regime, speed sweep was performed from 0.1 mm/s up to 1,024 mm/s.

To measure the contact film electric signal at various electric loads, an LCR metre was added to the ball on disc rig. Electric conducting accessories were designed to transfer the target film electric signal: the rotating steel ball was connected to the LCR metre through a copper coil; the glass disc was covered by a chromium

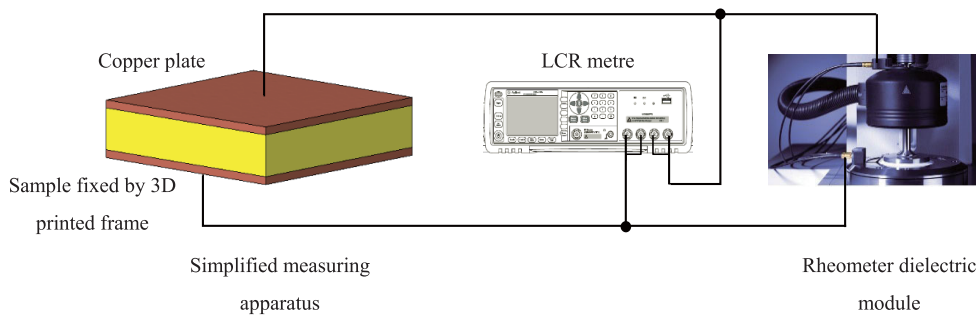

Fig. 1 Schematic drawing of the bulk grease impedance measuring set up.

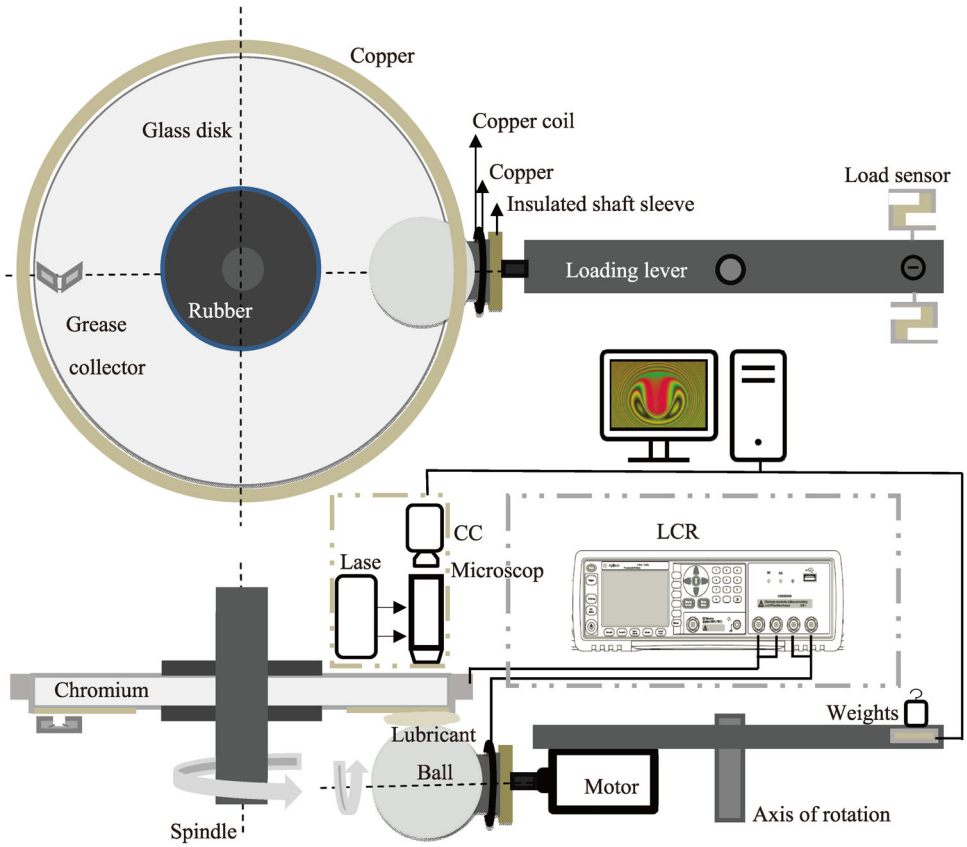

Fig. 2 Ball on disc rig coupled with electric loading and measuring circuit.

layer with specific thickness to ensure the simultaneous light transmission capability and electric conductivity; the glass disc was subsequently connected to the LCR metre by a copper ring around the disc perimeter. In this way, an electric circuit was constructed between the steel ball, contact zone, glass disc and the LCR metre, and the output film electric signal was rad through an oscilloscope (module DS1052E from RIGOL Technologies, not presented in the Fig. 2). The ball and disc were insulated from the rest of the structure to cut away the potential electric noise from the driving spindle or motor. To protect the electric driving systems from potential electric leakage, DC bias was not applied in the current study. Before each test, the background impedance including the glass disc, steel ball, connecting circuit, etc. was recorded at the designed frequency and subsequently removed from the film impedance value. More details on the test set up design and rig preparation can be found in the authors' previous work [35, 36]. The mechanical and electrical loading conditions for both bulk and tribological analysis in the current study are summarized in Table 2.

3 Results

3.1 Bulk grease electric impedance results

LCR frequency sweep results for fresh grease and bled oil are provided in Fig. 3(a) with the applied frequency as the horizontal line and the sample impedance as the vertical line. The corresponding Nyquist plotting for CG and NCG are provided in Fig. 3(b) with the real part Z_r as the horizontal line and imaginary part Z_i as the vertical line, from which an equalized electric circuit can be iterated.

Clearly, NCG and NCGBO show a capacitor dominating frequency response characteristics, namely the lubricant impedance drops with the frequency in a logarithm plot. This is in line with the common sense that grease is an isolating material and the bulk impedance measuring apparatus shown in Fig. 1 creates an equalling capacitor with grease as the dielectric

Table 2 Testing condition for grease analysis.

Ambient condition	Temperature (°C)	25
	Relative humidity (%)	36
Bulk grease analysis	Frequency sweep f (MHz)	10–1
	AC voltage amplitude (V)	1
	DC bias (V)	0–50
Tribological test	Entrainment velocity u_e (mm/s)	0.1–1,024
	Contact load F (N)	30
	Slide to roll ratio (SRR)	0
	Ball surface roughness $R_q\|_1$ (nm)	16.8
	Disc surface roughness $R_q\|_2$ (nm)	24
	Lubricant supply	Fully flooded
	Inlet grease track width w_{in} (mm)	2
	Inlet grease track height h_{in} (mm)	0.5
	Frequency F_{LCR} (kHz)	1, 100, 1,000
	Voltage amplitude (V)	1 (AC)

filling in-between. Interestingly, a very short plateau can be observed at low frequency regime (upto 200 Hz for NCG and upto 400 Hz for NCGBO), which is probably due to the existence of polarized composite such as additives, electrically active components, etc. Based on such behaviour, the impedance iteration (red curve in Fig. 3(b)) gives an R(CR) model.

CG, however, shows a different electric response: a resistive impedance can be found until the applied frequency reaches 10^5 Hz; afterwards, both CG and CGBO show a capacitive dropping impedance with the increasing frequency, falling to a similar impedance range as NCG. The impedance iteration (blue curve in the inset figure in Fig. 3(b)) gives an R(CR)(CR) model, which agrees with the electric mechanism for conductive grease [37]: when subjected to the electric field, electron current is transferred by the quantum-tunnelling effect between the neighbouring conductive particles, forming an intrinsic resistance [12]; if the conductive particles are too far away from each other, the quantum-tunnelling effect is eliminated and the dielectric bulk grease material (e.g., base oil, thickener, etc.) will create an equivalent capacitor in parallel. The combination of the resistive part and the capacitive part thus creates a macroscopic R(CR)(CR) performance. To characterize the CG electric behaviour, a "corner frequency" f_0 = 108,821 Hz is defined, where $Z_i = Z_r$, below which the resistant behaviour dominates and CG shows a lower impedance compared to NCG; from f_0 onwards, capacitive behaviour dominates and the difference between CG and NCG is no longer observable.

The equivalent impedance model shown in Fig. 3(b) indicates that when considering various frequencies, the electric performance for either CG or NCG cannot be simply represented by a capacitor, nor a resistor. Therefore, in the following analysis, volume impedance $\rho_v|_f$ (reciprocal of the specific conductivity) is selected as the major electric parameter:

$$\rho_v|_f = \frac{Z|_f \cdot A_p}{h_p} \tag{1}$$

where $Z|_f$ is the bulk grease impedance at the designed frequency f, A_p is the plate-plate geometry surface area, and h_p is the grease sample thickness.

Also noticed is that the bulk grease impedance is

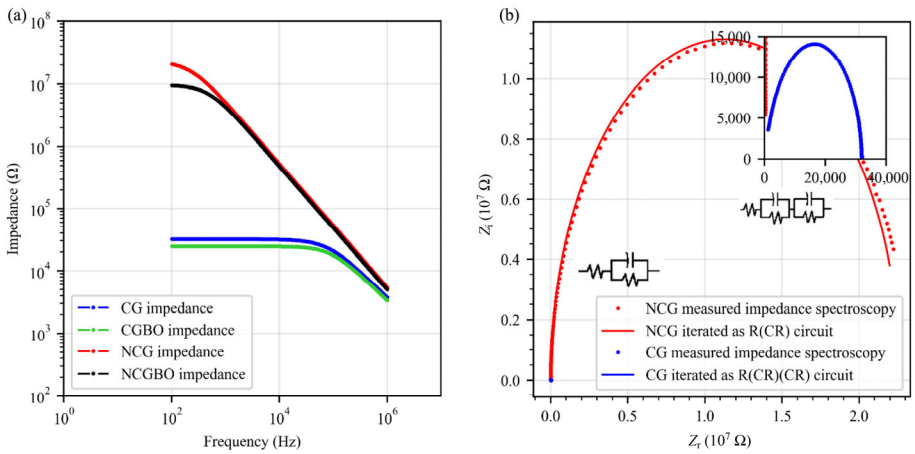

Fig. 3 (a) Frequency sweep plot and (b) impedance spectroscopy iteration for bulk lubricant (impedance measured using the rheometer)

higher than the bled oil for CG and NCG, especially at low frequency regimes. From this phenomenon, two points can be drawn: firstly, grease thickener also contributes to the impedance increment and this contribution is weakened with increasing frequency; secondly, for CG, the conductive agent does enter its bled oil, indicating an expected conductive contact film for CG lubrication.

In addition to frequency, voltage amplitude is another important factor for the electric loading. To protect the rheometer system, DC bias amplitude sweep was added to the simplified measuring apparatus as was shown in Fig. 1. The fresh grease response for DC bias sweep at different frequencies are given in Fig. 4. NCG is insensitive to the applied DC bias magnitude whilst CG's impedance exhibits an overshoot when the applied DC bias voltage exceeds a critical magnitude, ending up at a high impedance level. This critical DC bias magnitude is frequency dependent, namely CG tends to maintain its low impedance further at high frequency level. Besides, the impedance increment is less pronounced at high frequency range, for instance, CG impedance increases by 10^3 at 10 Hz during the DC bias sweep, whilst only by 20 times at 1 MHz. The comparison between Figs. 4(a) and 4(b) also demonstrates that after the impedance overshoot, CG gives even a higher impedance value than the NCG value.

Based on the previous work, working environment has a significant influence on grease properties [38]. Grease inside a motor bearing will be subjected to severe running conditions including high shear and elevated temperature. The electric response comparison between the fresh grease and its pre-treated sample (Table 1) are provided in Fig. 5 using the simplified measuring apparatus (as shown in Fig. 1) for trend analysis. Although the typical grease electrical response still holds after the ageing treatment, such procedure does change the grease impedance value. After baking at 120 and 150 °C in the open air, NCG grease impedance decreases, as shown by the downwards shifted blue and green dots (baked sample) compared to the black dots (fresh sample) in Fig. 5(a). On the contrary, for CG, elevated temperature results in a 65% impedance rising for baked CG (blue and green dots) compared to the fresh CG (black dots) in Fig. 5(b). According to the current results, pure shear has limited effect on the conductive grease electric performance. The FTIR spectrum shown in Fig. 6 indicates the chemical reaction of grease thickener at 150 °C, as shown in the green peak variation at 3,184 cm^{-1} and 1,600 cm^{-1} for both CG and NCG. This may have an influence on the overall grease electric performance. In addition, no base oil oxidation can be found from the FTIR results (1,730 cm^{-1}), which also tells that the bled oil test at 100 °C in Table 1 should be free from chemical reaction. Although the conducting agent is not given, there is no observable additive change in the FTIR results, which can be found from the fingerprint peaks comparison in the vicinity of 621–505 cm^{-1}.

The results show that the grease running history will have effects on its electrical impedance due to the potential change of chemical composition. Change of grease electric resistivity was also observed in the full bearing test in Ref. [29], and resulted in the initiation

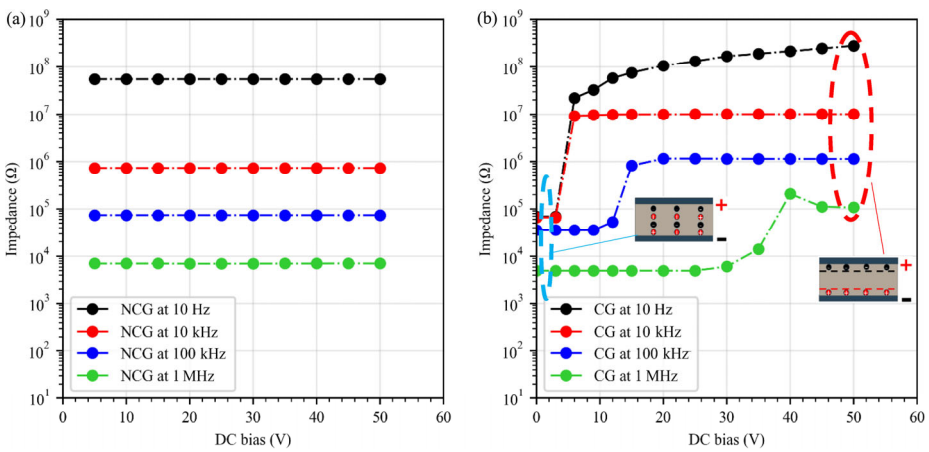

Fig. 4 (a) NCG and (b) CG bulk grease DC bias sweep at different frequencies (impedance measured using the simplified apparatus).

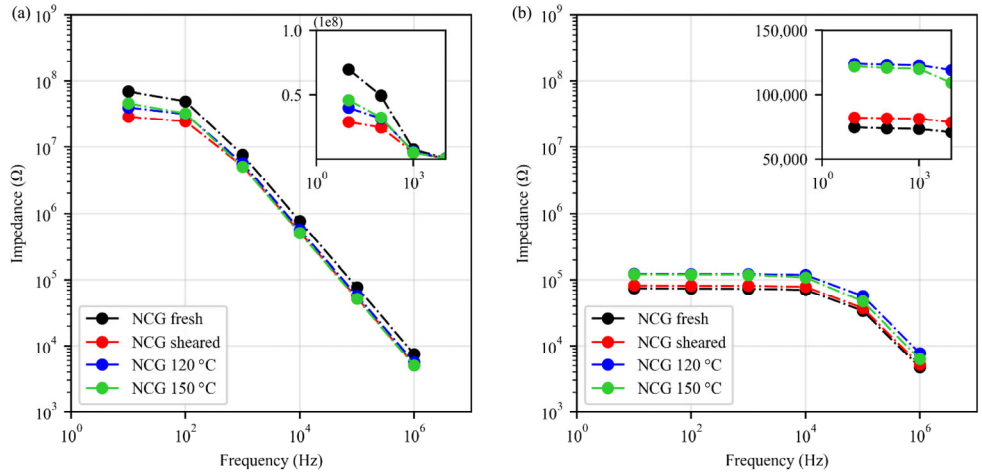

Fig. 5 (a) NCG and (b) CG bulk grease frequency sweep for different treatment (impedance measured using the simplified apparatus)

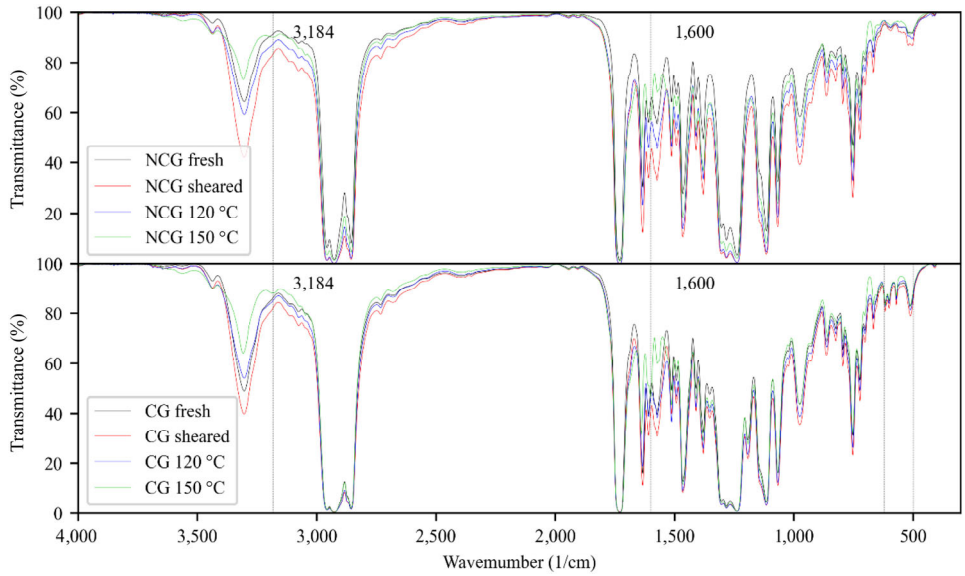

Fig. 6 FTIR comparison for aged (a) NCG and (b) CG.

of electric erosion. The CG conductivity is expected to serve the bearing lifespan, but the running condition, such as elevated temperature, or possibly contaminant invasion (not investigated in this paper yet) may change the conductive agent behaviour. This will introduce a concept as "conductivity life", the bearing users should pay attention to the bearing working environment and its influence on the CG electric characteristic to prevent the fast loss of the CG conductivity life.

3.2 Film thickness and film impedance results

Inside a bearing, the lubricant electric performance is highly dependent on the film layer in the contact area determined by the mechanical running condition and the electric loading condition. The lubricant film thickness profile was firstly collected between a steel ball and a chromium coated glass disc using the in-house made ball on disc test rig following the speed sweep test provided in Table 2. The contact central film thickness h_{cen} for CG, NCG, CGBO, NCGBO and typical grease film profiles at different lubricant regimes are presented in Fig. 7(a). As expected, CG and NCG grease show similar film thickness variation due to similar grease composites and a "V-shaped" film thickness behaviour can be observed. Such results are in line with the grease film thickness variation as in Ref. [39]. Besides, the results also illustrate that the conductive agent in CG has no observable effect on the film thickness construction.

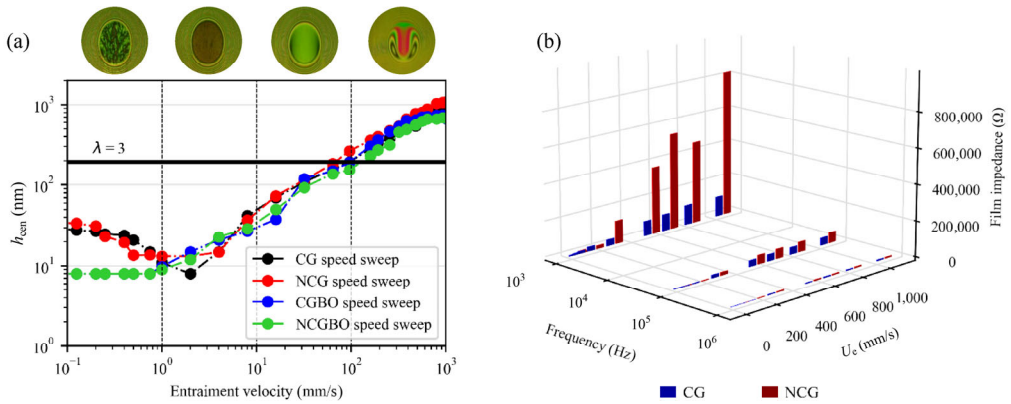

Fig. 7 (a) Speed sweep CG/NCG central film thickness h_c and (b) film impedance at different frequencies.

The lubrication regime for CG and NCG can be roughly estimated based on the speed sweep film thickness, characterized by the classic lambda value λ (defined as the ratio of the minimum film thickness over the composite roughness of the contact surfaces). The mixed lubrication regime can be determined by entrainment velocity $u_e \leq 128$ mm/s, where $\lambda \leq 3$ [40]. Afterwards, full film separation is constructed, and direct asperity contact is largely reduced.

At each speed, in line with the film profile collecting, the contact film impedance between the ball and disc was measured using the LCR metre. Three typical electric frequencies were selected: 1 kHz, 100 kHz, and 1 MHz, to cover the full CG grease electric curve, i.e., the low impedance plateau, corner frequency, and capacitive impedance dropping area shown in Fig. 3(a). The measured film impedance at different entrainment velocities and electric frequencies are presented in Fig. 7(b) for CG (blue bar) and NCG (red bar).

Under full lubricant supply condition, with increasing speed, the constructed film thickness gives rise to a climbing film impedance. According to Fig. 7(a), CG and NCG show similar film thickness behaviour, hence the difference in CG and NCG film impedance should be ascribed to the lubricant intrinsic electric property. When the film is sufficiently thick to separate the two contact surfaces ($u_e > 128$ mm/s), observable film impedance difference between CG and NCG can be found, especially at low frequency range, e.g., 1 kHz. This verifies the entrance of conductive agent into the contact zone for CG (at least in this full lubricant supply condition) and confirms the earlier bulk CG analysis: at low electric frequency, CG is dominated by resistant property and a conductive film can be built. When the applied frequency exceeds the CG corner frequency f_0, CG film impedance clearly show a decreasing tendency, where capacitive property prevails, and the film impedance difference between CG and NCG is no longer observable. Also noticed is that in the mixed lubrication regime ($u_e < 128$ mm/s), the film impedance difference between CG and NCG is not noticeable because of the occasional electric short circuit generated by the direct asperity contacts.

3.3 Comparison between calculated and measured film impedance

As Fig. 7(b) displays, a frequency dependent film impedance is observed for CG and NCG, showing a similar trend as the bulk grease frequency dependency in Fig. 3(a). To understand the connection between the bulk grease behaviour and that inside the contact zone, film impedance is calculated by taking use of the bulk lubricant volume impedance $\rho_v|_f$ from Fig. 3(a), the grease track geometry from grease collector (w_{in} and h_{in} in Table 2), and the EHL lubricant film thickness profile h.

To calculate the film profile inside the contact zone, the lubricant piezo-viscous behaviour is required. Here the bled oil pressure–viscosity coefficient α is calculated following Foord's method [41], making use of the empirical central film thickness h_c data in Fig. 7(a) in the range of 1 mm/s $< u_e <$ 640 mm/s, where a piece-wise linear plotting can be found between h_c and u_e, using Hamrock and Dowson equation for a fully flooded point contact [42]. The parameters used in Hamrock and Dowson equation are calculated from the tribological test condition in Table 2 and the

EHL parameters in Table 3. The dimensionless CGBO and NCGBO film parameter $H\left(H=\frac{h_c}{R}\right)$ and the speed parameter $U\left(U=\frac{u_e\eta_0}{(E^*R)}\right)$ are scattered in Fig. 8, where $E^*=2\Big/\left(\frac{1-v_1^2}{E_1}+\frac{1-v_2^2}{E_2}\right)$, $R=1\Big/\left(\frac{1}{R_x}+\frac{1}{R_y}\right)$. The curve fitting gives the bled oil pressure–viscosity coefficient as $\alpha=2.6\times10^{-8}$ Pa^{-1} for CGBO and $\alpha=2.1\times10^{-8}$ Pa^{-1} for NCGBO. The EHL lubricant film thickness profile h inside the contact zone is thus achieved by numerically solving the isothermal Reynold's equation, pressure field, pressure–viscosity equation, and pressure–density equation using multigrid numerical method [43] and the calculated central film thickness for each speed shows a good agreement as the measured results h_c.

Table 3 EHL parameters.

Steel ball radius in x and y directions	R_x and R_y (m)	0.013
Elastic moduli for steel ball	E_1 (Pa)	2.2×10^{11}
Elastic moduli for glass disc	E_3 (Pa)	2.2×10^{10}
Poisson ratio for steel ball	u_1	0.30
Poisson ratio for glass disc	u_2	0.21

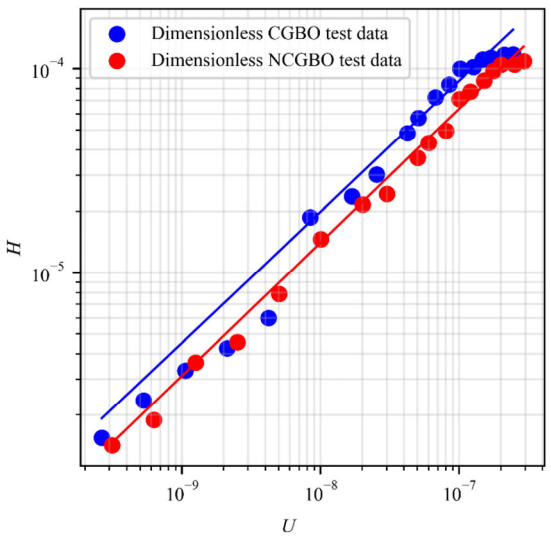

Fig. 8 Dimensionless bled oil film thickness.

The contact impedance calculation is on the foundation of lubricant distribution at the contact area and thus is divided into four sections shown in Fig. 9. (1) The Hertzian contact section z_{Hertz}, namely, the EHL film thickness profile section. (2) The inlet section z_{inlet}. Considering the current fully lubricant supply condition, the computed domain is set up to the grease filling boundary between the ball and glass disc surface, namely the position where the surface separation is bigger than the inlet grease track height h_{in}(0.5 mm). (3) The two contact side sections z_{side}, determined by the grease track boundary, namely, the track width up to $w_{\text{in}}=2$ mm. (4) The outlet section z_{outlet}, where the computed domain is set the same as the inlet area, but the cavitation zone is determined as a quarter of the total area surrounding the outlet area until the cavitation width reaches 2 times of the Hertzian contact width (lubricant replenishment is not considered in the current flat disc case) [44]. In the cavitation zone, the lubricant is estimated to be split into two equal thicknesses $0.5h_c$ adhering to the contact surfaces, and the rest of the gap is filled with air [44]. Therefore, the cavitation impedance is equal to two film impedance $z_{0.5h_c}$ and one air impedance z_{air} in a series arrangement. The equivalent electric circuit for the contact impedance is provided in Fig. 9(b). In the current approach, only the lubricant film impedance is calculated and the two contact surfaces are assumed to be perfectly smooth, and thereby the resistance component due to potential asperity contact is not considered.

The calculated contact film impedance z_{film} is achieved by summarizing the unit lubricant impedance $Z_{i,j}$ over the computing zone in a parallel arrangement.

$$\frac{1}{z_{\text{film}}}=\frac{1}{z_{\text{inlet}}}+\frac{1}{z_{\text{Hertz}}}+\frac{1}{z_{\text{side}}}+\frac{1}{z_{\text{outlet}}}=\sum_{i,j}\frac{1}{z_{i,j}} \tag{2}$$

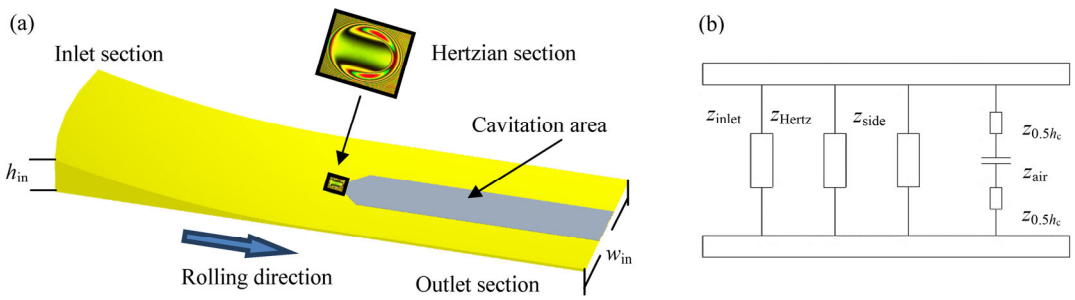

Fig. 9 (a) Film impedance calculating domain and (b) the equivalent electric circuit

$z_{i,j}$ in the lubricant filling area is

$$z_{i,j} = \frac{\rho_v\big|_f \cdot h_{i,j}}{A_{i,j}} \tag{3}$$

where i and j are the node indexes in x and y computing direction. The unit impedance $z_{i,j}$ at each computing node is obtained from the frequency dependent volume impedance $\rho_v\big|_f$, and the calculated lubricant thickness $h_{i,j}$ over each computing grid area $A_{i,j}$ [45]. The optical interferometry film profile in Fig. 7(a) indicates that inside the Hertzian contact zone, after $u_e > 1$ mm/s, bled oil is the major material contributing to the film construction, and thus for z_{Hertz}, bled oil volume impedance is used; for the rest surroundings, i.e., z_{side} and z_{inlet}, bulk grease volume impedance is used.

At the cavitation zone, because the air is considered as a capacitance directly, for each computing grid, the cavitation impedance is calculated from the imaginary part $Z_{i,j}\big|_{\text{i}}$ and the real part $Z_{i,j}\big|_{\text{r}}$.

$$z_{i,j} = \sqrt{Z_{i,j}\big|_{\text{i}}^{\,2} + Z_{i,j}\big|_{\text{r}}^{\,2}}, \tag{4}$$

where $Z_{i,j}\big|_{\text{i}}$ covers the imaginary part of the film layer: $2\times\left|z_{0.5h_c}\right|\cdot\sin\theta$ (θ is the bled oil impedance angle) and the capacitive air impedance $\left(2\pi f\dfrac{\varepsilon_r\cdot\varepsilon_0\cdot A_{i,j}}{h_{i,j}-h_c}\right)^{-1}$ ($\varepsilon_0 = 8.85\times10^{-12}\,\dfrac{F}{m}$, $\varepsilon_r = 1.0$, and $h_{i,j}$ is the contact surface separation); $Z_{i,j}\big|_{\text{r}}$ is the real part of the film layer: $2\times\left|z_{0.5h_c}\right|\cdot\cos\theta$.

The calculated film impedance z_{film} at 1 kHz, 100 kHz, and 1 MHz, is then compared to the measured lubricant film impedance value in Figs. 10(a) and 10(b), where the calculated impedance is presented in dashed line and the measured impedance is presented in boxplot at each speed and frequency. Also plotted are the film impedance angle in Figs. 10(c) and 10(d), where the dashed line presents the impedance angle from bulk lubricant analysis, and the boxplot presents the measured film impedance angle at each specific frequency and speed. The film impedance angle gives an indication of the contact status: impedance angle close to 0° tells a resistive film behaviour, and impedance angle close to –90° tells a capacitive film.

4 Discussion

The electric and tribological behaviour of CG is presented by comparing it with NCG. The causes of differences in the results are analyzed and discussed in this section.

In Fig. 4, an abrupt impedance jump is found for CG at elevated DC magnitude. The current hypothetical explanation for this impedance jump is electric polarization induced by the high voltage DC electric field, where the conductive particles are separated and accumulated in the vicinity of two plates (see the schematic drawing of the conductive agent movement at different DC amplitude level in Fig. 4(b)), leading to the loss of conductive agent mobility in the bulk grease volume, and the increment of CG impedance. This is predominant in the low frequency regime, where the quantum-tunnelling path works. At high frequency regime, capacitive behaviour dominates, and such impedance jumping will be weakened. To sum up, a DC voltage threshold value is observed, above which CG will lose its conductivity, which may suggest certain application boundary for CG grease.

In Fig. 10, the first remarkable difference can be found at low speed regime: when $u_e < 128$ mm/s, for both CG and NCG, the measured film impedance shows a considerable negative deviation from the calculated value, and the film impedance angle is close to zero, giving a resistive contact film behaviour independent of the applied frequency. This is in line with the calculated film separation λ value shown in Fig. 7(a), indicating that the film impedance is highly dependent on the lubrication regime: when the film separation is not sufficient, the periodic direct asperity contact results in an electric short circuit, thereby a rather small resistive contact impedance, independent of the applied electric frequency. Since the current calculation model does not take the surface roughness into account, and thus the impact of direct asperity contact on the film impedance behaviour cannot be reflected. For a grease lubricated bearing, running environments such as starvation, high temperature and limited bleeding may lead to thinner film, resulting in substantial surface contact [46] and the

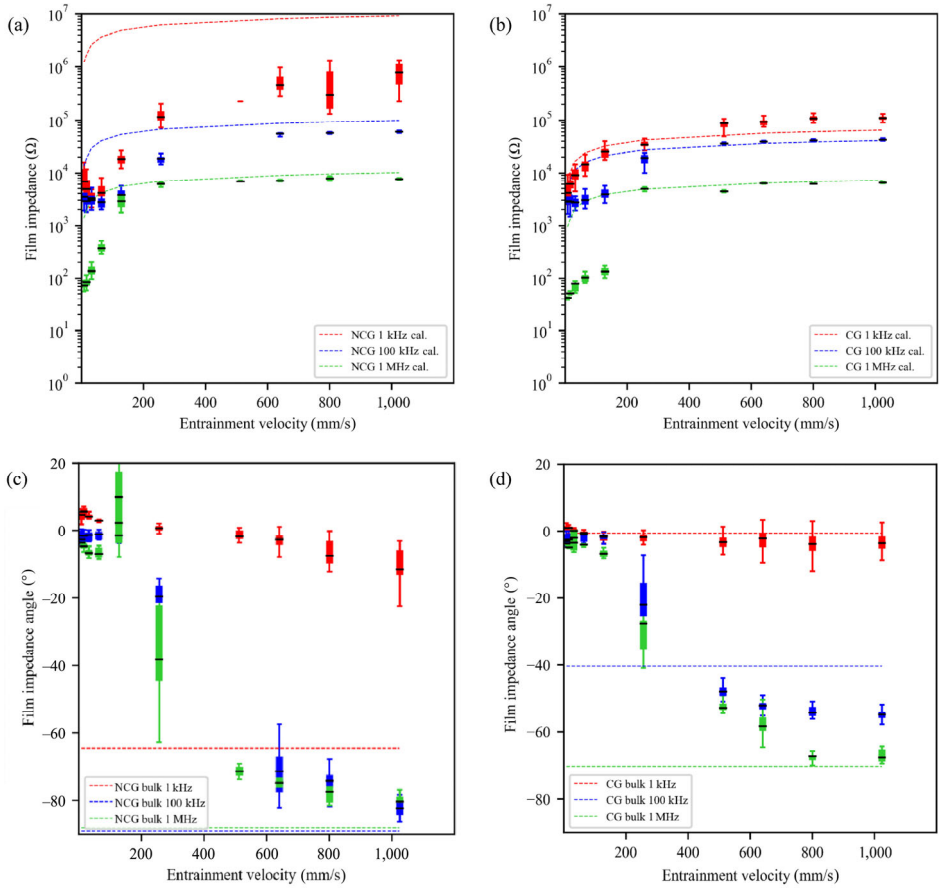

Fig. 10 Comparison between measured and calculated film impedance for (a) NCG and (b) CG; and comparison between film impedance angle and bulk grease impedance angle for (c) NCG and (d) CG.

accumulated electric load will be transferred away through an ohmic current. In such case, the CG and NCG difference will no longer exist. This may be the explanation for Tischmacher's full bearing test results [47], where after 40-hour running (when the churning phase might finish), the conductive grease lubricated bearing showed a similar electric signal as the non-conductive grease lubricated bearing.

When a sufficient film separation is constructed, the lubricant electric parameter will play a role inside the contact zone. As expected, CG shows lower film impedance compared to NCG over the tested frequency spectrum, and despite the data fluctuation, the measured CG film impedance agrees with the calculated value. The CG contact film impedance angle falls in similar range as the bulk CG analysis, i.e., a resistive film is constructed at 1 kHz; after the "corner frequency" f_0, a capacitive film is built at 100 kHz and 1 MHz. Similar behaviour is also observed for NCG at high frequency regime.

However, at 1 kHz, the NCG generates a resistive film with lower impedance value compared to the calculated results, as shown by the film impedance and impedance angle comparison in Figs. 10(a) and 10(c). The current explanation is the influence of pressure and measuring distance on the lubricant electric parameters. According to the bulk impedance results in Fig. 3, NCGBO provides a very short resistive impedance plateau by 400 Hz which was attributed to polarized additives or the potential existence of active electrons. This bulk lubricant impedance is measured at open air; whilst the lubricant inside the contact zone is subjected to 0.5 GPa contact pressure (Table 2). According to the literature, lubricant dielectric constant is a function of pressure dependent density following either Clausius–Mossotti equation [48] or Schmidt's equation [49]. The high contact pressure might affect the lubricant electric properties and thereby the film impedance. In addition, the contact film thickness is on a nano

to micron metre scale, and in such a small distance, quantum-tunnelling effect might take place between the dissolved polarized additives in NCG as well, such as potential extreme pressure (EP), anti-oxidation, anti-corrosion additives, etc., and a resistive current bridge might be built at low frequency regime, giving a relatively low film impedance value. With increasing electric frequency, capacitive behaviour dominates (indicated by a negative impedance angle shown in Fig. 10(c)) and the measured contact film impedance falls in similar range as the calculated data again. Unfortunately, the author cannot validate these hypotheses by far, nor can we conclude whether the NCG film electrical performance can be promoted to other general greases. Besides, the assumption used in the impedance calculating model may also introduce the value deviation. The current model considers only the film thickness resulted impedance, but as the asperity contact is a matter of probability, even when full film separation is built ($\lambda > 3$), potential asperity contact may still take place and change the film impedance. Also, at the outlet cavitation area, two equal film separation with $0.5h_c$ thickness is used for the calculation may lead to deviation as well. More detailed exploration is expected to study the influence of contact parameters on the lubricant electrical performance and the corresponding contact impedance.

5 Conclusion

The electrical and tribological properties of a conductive grease CG have been investigated and compared to its non-conductive counterpart NCG. Electric and mechanical loadings are applied when analysing the grease lubricity and contact film impedance. Based on the experimental and calculated results, the observations are summarized as follows.

1) Different from the conventional lubricant, the selected CG product cannot be equalized as a capacitor nor a resistor directly, but a R(CR)(CR) arrangement according to the impedance spectroscopy analysis. When the applied frequency exceeds a corner frequency f_0 for CG, the impedance difference between CG and NCG will be eliminated, thus the resistive low impedance plateau for CG should cover the electric frequency range for the target field application. Also, a large voltage amplitude will result in an irreversible loss of CG conductivity.

2) Working environments, especially chemical reaction at elevated temperatures will change the grease impedance and conductivity. Therefore, the conductive grease should be developed not only to provide good lubricity and oil supply, but also to guarantee that the conductive agent, with a reliable "conductive life" considering the working condition, is capable to enter and function well inside the contact zone.

3) The contribution of CG to film impedance is closely related to the contact lubrication condition. In the mixed lubrication regime, the potential short circuit due to asperity direct contact will eliminate the impedance difference between CG and NCG and give a resistive film. When the contact surfaces are fully separated by the lubricant film, the bulk CG electric behaviour is observed inside the contact zone as well: a relatively low resistive film at low frequency regime, where the accumulated electric energy between the contact surfaces can be dissipated; and a capacitive film at high frequency regime, where CG will provide similar behaviours as NCG.

4) Bulk grease parameters, e.g., the dielectric constant, volume impedance or specific conductivity, may be affected by the contact parameters such as contact pressure, flash temperature, etc. Therefore, empirical parameters based on the combined tribological and electrical test are needed in the case of accurate film impedance prediction.

Acknowledgement

The author would like to thank Weihua QIAN, Yunfei PAN and He ZHU for their kind supports and permission to publish this paper. The author would also thank Guillermo MORALES and Liang GUO for their proof review and valuable recommendations.

Declaration of competing interest

The authors have no competing interests to declare that are relevant to the content of this article.

References

[1] Kalaiselvi J, Srinivas S. Bearing currents and shaft voltage reduction in dual-inverter-fed open-end winding induction motor with reduced CMV PWM methods. *IEEE Trans Ind Electron* **62**(1): 144–152 (2015)

[2] Robles E, Fernandez M, Ibarra E, Andreu J, Kortabarria I. Mitigation of common mode voltage issues in electric vehicle drive systems by means of an alternative AC-decoupling power converter topology. *Energies* **12**(17): 3349 (2019)

[3] He F, Xie G X, Luo J B. Electrical bearing failures in electric vehicles. *Friction* **8**(1): 4–28 (2020)

[4] Zika T. Electric discharge damaging in lubricated rolling contacts. Ph.D. Thesis. Vienna (Austria): Vienna University of Technology, 2010.

[5] Oliver J, Guerrero G, Goldman J. Ceramic bearings for electric motors. In: Proceedings of the IEEE-IAS/PCA Cement Industry Conference (IAS/PCA CIC), Toronto, Canada, 2015: 1–11.

[6] Schiferl R F, Melfi M J. Bearing current remediation options: Sources, investigative measurements, and installation modifications to reduce damage as a result of bearing currents. *IEEE Ind Appl Mag* **10**(4): 40–50 (2004)

[7] Trelleborg. Turcon MC1 and MC2 materials-uniquely electrically conductive, 2020. Available at https://www.trelleborg.com/zh-cn/seals/products-and-solutions/latest-innovations/turcon-mc1-mc2.

[8] Chen Y, Jha S, Raut A, Zhang W Y, Liang H. Performance characteristics of lubricants in electric and hybrid vehicles: A review of current and future needs. *Front Mech Eng* **6**: 571464 (2020)

[9] Ge X Y, Xia Y Q, Shu Z Y. Conductive and tribological properties of lithium-based ionic liquids as grease base oil. *Tribol Trans* **58**(4): 686–690 (2015)

[10] Tu C J, Chen Z H, Xia J T. Thermal wear and electrical sliding wear behaviors of the polyimide modified polymer-matrix pantograph contact strip. *Tribol Int* **42**(6): 995–1003 (2009)

[11] Holm R. *Electric Contacts; Theory and Application*. Heidelberg (Germany): Springer Berlin, 1967.

[12] He L, Chen Y, Tian F, Zeng J, Yang X, Ye Z. Research progress and application of conductive grease. *J Harbin Univ Sci Technol* **29**(2) (2022)

[13] Cao Z F, Xia Y Q, Chen C, Zheng K, Zhang Y. A synergetic strategy based on laser surface texturing and lubricating grease for improving the tribological and electrical properties of Ag coating under current-carrying friction. *Friction* **9**(5): 978–989 (2021)

[14] Fan X Q, Xia Y Q, Wang L P. Tribological properties of conductive lubricating greases. *Friction* **2**(4): 343–353 (2014)

[15] Kuo M C, Hoover W R, Akkala M W, Mehlhorn W L. Conductive greases and methods for using conductive greases in motors. U.S. Patent 0062350A1, Mar. 2005

[16] Wang Z Y, Xia Y Q, Liu Z L, Wen Z Z. Conductive lubricating grease synthesized using the ionic liquid. *Tribol Lett* **46**(1): 33–42 (2012)

[17] Cao Z F, Xia Y Q, Ge X Y. Conductive capacity and tribological properties of several carbon materials in conductive greases. *Ind Lubr Tribol* **68**(5): 577–585 (2016)

[18] Ge X Y, Xia Y Q, Shu Z Y, Zhao X P. Conductive grease synthesized using nanometer ATO as an additive. *Friction* **3**(1): 56–64 (2015)

[19] Graves S M, Rodriguez D A S, Grendahl T N, Hain A. Electric motor rotor discharge protection. USA. Patent 11088582, Nov. 2021.

[20] Kempski A. Capacitively coupled discharging currents in bearings of induction motor fed from PWM (pulsewidth modulation) inverters. *J Electrost* **51–52**: 416–423 (2001)

[21] Lugt P M. *Grease Lubrication in Rolling Bearings*. John Wiley & Sons Ltd., 2012.

[22] Luo J B, Shen M W, Wen S Z. Tribological properties of nanoliquid film under an external electric field. *J Appl Phys* **96**(11): 6733–6738 (2004)

[23] Xie G X, Guo D, Luo J B. Lubrication under charged conditions. *Tribol Int* **84**: 22–35 (2015)

[24] Xie G X, Luo J B, Guo D, Liu S H. Nanoconfined ionic liquids under electric fields. *Appl Phys Lett* **96**(4): 043112 (2010)

[25] Luo J B, He Y, Zhong M, Jin Z M. Gas bubble phenomenon in nanoscale liquid film under external electric field. *Appl Phys Lett* **89**(1): 013104 (2006)

[26] Xie G X, Luo J B, Guo D, Liu S H, Li G. Damages on the lubricated surfaces in bearings under the influence of weak electrical currents. *Sci China Technol Sci* **56**(12): 2979–2987 (2013)

[27] Chiou Y C, Lee R T, Lin C M. Formation criterion and mechanism of electrical pitting on the lubricated surface under AC electric field. *Wear* **236**(1–2): 62–72 (1999)

[28] Raadnui S, Kleesuwan S. Electrical pitting wear debris analysis of grease-lubricated rolling element bearings. *Wear* **271**(9–10): 1707–1718 (2011)

[29] Har P. Investigation of damaged rolling-element bearings and deterioration of lubricants under the influence of electric fields. *Wear* **176**(2): 151–161 (1994)

[30] Gonda A, Capan R, Bechev D, Sauer B. The influence of lubricant conductivity on bearing currents in the case of rolling bearing greases. *Lubricants* **7**(12): 108 (2019)

[31] Cao Z F, Xia Y Q, Xi X. Nano-montmorillonite-doped lubricating grease exhibiting excellent insulating and tribological properties. *Friction* **5**(2): 219–230 (2017)

[32] Suzumura J. Prevention of electrical pitting on rolling bearings by electrically conductive grease. *QR RTRI* **57**(1): 42–47 (2016)

[33] DL/T 373-2019. Technical conditions of conductive paste. 2019.

[34] US-ASTM. ASTM D2624-09. Standard test methods for electrical conductivity of aviation and distillate fuels. 2009.

[35] Zhou Y, Han B, Pan Y, Chong H, Lu L, Li X, Bai Q, Liu, J. A tribological measuring method combining both electric impedance and optical interferometry film profile. Patent in process.

[36] Chong H, Zhou Y X, Liu J J, Yang P, Han B, Li X M. Measurement of lubricating film thickness by combing electrical capacitance and optical interferometry method. *Lubication Engineering* **48**(2):135–141(2022)

[37] Reddy A B, Shah F U, Leckner J, Rutland M, Glavatskih S. On electric conductivity of greases. *Research Square Preprint* https://doi.org/10.21203/rs.3.rs-1296562/v1 (2022)

[38] Zhou Y X, Bosman R, Lugt P M. A master curve for the shear degradation of lubricating greases with a fibrous structure. *Tribol Trans* **62**(1): 78–87 (2019)

[39] Cen H, Lugt P M, Morales-Espejel G. On the film thickness of grease-lubricated contacts at low speeds. *Tribol Trans* **57**(4): 668–678 (2014)

[40] Maru M M, Tanaka D K. Consideration of stribeck diagram parameters in the investigation on wear and friction behavior in lubricated sliding. *J Braz Soc Mech Sci & Eng* **29**(1) (2007)

[41] Foord C A, Hammann W C, Cameron A. Evaluation of lubricants using optical elastohydrodynamics. *A S L E Trans* **11**(1): 31–43 (1968)

[42] Hamrock B J, Dowson D. Elastohydrodynamic lubrication of elliptical contacts for materials of low elastic modulus I—Fully flooded conjunction. *J Lubr Technol* **100**(2): 236–245 (1978)

[43] Yang P R. *Numerical Analysis of Fluid Lubrication*. Beijing: National Defense Industry Press, 1998.

[44] Jablonka K, Glovnea R, Bongaerts J. Evaluation of EHD films by electrical capacitance. *J Phys D*: *Appl Phys* **45**(38): 385301 (2012)

[45] Gemeinder Y, Schuster M, Radnai B, Sauer B, Binder A. Calculation and validation of a bearing impedance model for ball bearings and the influence on EDM-currents. In: Proceedings of the International Conference on Electrical Machines (ICEM), Berlin, Germany, 2014: 1804–1810

[46] Mérieux J S, Hurley S, Lubrecht A A, Cann P M. Shear-degradation of grease and base oil availability in starved EHL lubrication. *Tribol Ser* **38**: 581–588 (2000)

[47] Tischmacher H, Gattermann S. Investigations on bearing currents in converter-fed electrical motors. In: Proceedings of the International Conference on Electrical Machines, Marseille, France, 2012: 1764–1770

[48] Jablonka K, Glovnea R, Bongaerts J. Quantitative measurements of film thickness in a radially loaded deep-groove ball bearing. *Tribol Int* **119**: 239–249 (2018)

[49] Anatoly Z, Steffen P, André H, Marcel N, Eckhard K. A comparison of an analytical and a numerical approach to calculate the electrical capacitance of rolling element bearings. In: Proceedings of the 4th International FVA-Conference, Würzburg, Germany, 2022: 8–15.

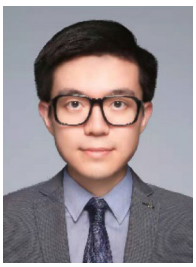

Yuxin ZHOU. He is a tribology researcher at SKF (Shanghai) Automotive Technologies Co., Ltd., China. He received his master's degree from Imperial College London, UK, in 2013 and received his Ph.D. degree from University of Twente, the Netherlands, in 2018. His research interests include contact film, grease, bearing life and performance, and lubricant condition monitoring.

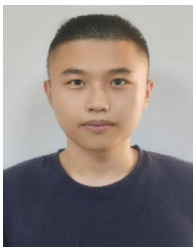

Jinjie LIU. He is currently Ph.D. candidate at Qingdao University of Technology, China. He received his master's degree from School of mechanical engineering, Qingdao University of Technology, China, in 2023. His research interest focuses on lubrication and electrical corrosion.